REDOX DEPOSITION OF MnO_2 NANOPARTICLES ON RICE HUSK BASED ACTIVATED CARBON AS HIGH-PERFORMANCE ELECTRODE MATERIAL FOR PSEUDO-CAPACITORS

Abdul Hayat Kasim[1], M. Zakir[1*], Musa Ramang[1], Bannu Abdussamad[2]

[1] Department of Chemistry, Faculty of Science, Hasanuddin, University, Indonesia
[2]Department of Physics, Faculty of Science, Hasanuddin, University, Indonesia
Corresponding author: muhammadzakir@gmail.com

Abstract. MnO_2/rice husk activated carbon (KASP) nanocomposites have been synthesized by directly reducing $KMnO_4$ with KASP in an aqueous solution. XRD diffraction data showed a broad and typical peak MnO2 at 37 2theta as an indicator that the compound obtained are amorphous. Fluorescence data (XRF) also supports that after addition of KMnO4 to the rice husk based acticated carbon solution concurrently MnO2 nanoparticles deposition takes place on the surface of KASP. It is found that the morphologies of MnO_2 grown on KASP can be tailored by varying the reaction ratio of KASP and $KMnO_4$. A pseudo-capacitor with high energy density was fabricated by using MnO_2/RHAC nanocomposite as positive electrode and activated carbon as negative electrode in 1 M Na_2SO_4 aqueous electrolyte. The pseudocapacitor can be cycled reversibly in the cell voltage of 0.2 V, and delivers a specific capacitance of *25.4 mF* g^{-1} (based on the total mass of active electrode materials of 9.4 mg), which is much higher than that of supercapacitor without MnO_2 deposition (*8.6* μF g^{-1}), or there is significance increase in capacitance (± 3000 times). We obtained also that supercapacitor's electrode developed from rice husk based activated carbon has a better performance compared to one developed from commercially activated carbon material. Such a better electrochemical performance makes nanocomposite of MnO2/KASP as a promising electrode material for supercapacitors.

Key words: *pseudo*-capacitor, rice husk based activated carbon, MnO2 nanoparticles

INTRODUCTION

Pseudo-capacitor, another varian of supercapacitors or electrochemical capacitors have attracted great attention as a promising energy storage device due to their higher power density, longer cycle life than batteries, and higher energy density than conventional dielectric capacitors [1-3]. Recently, extensive work has been focused on ways to enhance both the energy and power density of supercapacitors [4-6]. According to the following equation:

$$E = \frac{1}{2} CV^2 \quad (1)$$

The enhancement in energy (E) can be achieved by increasing the specific capacitance (C) and/or broadening the cell voltage (V). The capacitance depends on the electrode material used, whereas the cell voltage is determined by the stability window of the electrolyte and also the electrode material characteristics. The latter can be achieved with organic electrolytes that are characterized by a wide electrochemical stability window (from 2 to 4 V) [7-10]. However, organic electrolytes are quite expensive, highly toxic, flammable, and require cell construction in air-free atmosphere. Aqueous electrolytes can work in a voltage window around 1 V (the thermodynamic window of water is 1.23 V) with a relatively low equivalent series resistance (ESR) [11,12]. However, the cell voltage is too low and should be improved in view of practical applications. A promising way to increase the cell voltage in aqueous electrolytes is to develop asymmetric supercapacitors, which consist of a pseudocapacitive or battery-type positive electrode and a high surface-area carbon negative electrode [4]. The asymmetric design offers the advantages of both supercapacitors (rate, cycle life) and batteries (energy density) [13]. Recently, various asymmetric aqueous supercapacitors, such as activated carbon (AC)//$LiMn_2O_4$ [14], AC//$Ni(OH)_2$ [15], AC//V_2O_5 [16], AC//MnO_2 [17e28], and Fe_3O_4//MnO_2 [29] have been explored.

MnO_2 is considered as one of the most promising electrode materials for supercapacitors owing to its low cost and environmental friendliness [30e36]. However, MnO_2 shows a low electrical conductivity (105 to 106 S cm1) [37]. High conductive materials such as activated carbon were combined with MnO_2 to improve the electrical conductivity of MnO_2-based electrodes [38,39]. However, the electrochemical performances of MnO_2 composites were tested in a three-electrode system with a narrow voltage window (about 1 V) in most of previous works. Very recently, Gao et al. prepared MnO_2/AC composite by physical mixing and fabricated an asymmetric supercapacitor with the two electrodes of MnO_2/AC composite and AC. An energy density of 18.7 Wh

kg1 was obtained for such supercapacitor [40].

Herein, we reported on the synthesis of MnO_2/KASP (Rice Husk Based Activated Carbon) nanocomposites in a solution containing KMnO4 and KASP through the heterogeneous nucleation of MnO_2 onto the surface of KASP. The morphologies of MnO_2 grown on KASP were changed from nanorods to nanoparticles while decreasing the reaction ratio of RHAC/KASP. Such hierarchical structures can improve the electrochemical performance relative to conventional powder-composite MnO_2/KASP electrodes. A pseudo-capacitor manufactured with MnO_2/KASP nanocomposite as the positive electrode and RHAC as the negative electrode can be reversibly charged/discharged at a maximum cell voltage of 2 V in aqueous electrolyte, delivering a higher energy density in comparison with a MnO_2/KASP pseudo-capacitor.

MATERIAL AND METHODS

All chemicals used in this study are of analytical grade, and used without further purification. Capacitor-grade activated carbon with a specific surface area of about 2500 m2 g1 measured by the BET method was purchased from Intraco Co., Ltd (Makassar, Indonesia).

Manganese oxide/KASP nanocomposites were synthesized by chemical precipitation in an aqueous solution containing $KMnO_4$ and KASP. In a typical process, 0.6 g of KASP was added into 100 mL of 0.05 M $KMnO_4$ solution. Subsequently, the mixture was stirred under thermostatic bath at 95 C and refluxed until completely colorless. The products were filtered and washed several times with deionized water, then dried at 60 C in the air for 12 h. The products were denoted as S1, S2, and S3 for the addition of 0.6, 0.4, and 0.2 g of RHAC, respectively.

X-ray diffraction (XRD) measurement was performed on a Shimadzu XRD-6000 diffractometer with Cu Ka radiation. The particle morphology of the sample was investigated by means of field emission scanning electron microscopy (FESEM) with a JEOL JSM-6700F microscope. C, H and N microanalysis was recorded on an Elementar Vario El elemental analyzer. Thermogravimetry (TG) analysis was carried out on a Perkin Elmer Diamond analyzer with N2 gas. Samples were heated from 50 to 800 C at a rate of 10 C min^{-1}.

The working electrode was prepared by mixing 70 wt% active material, 20 wt% acetylene black and 10 wt% poly(vinylidene fluoride) (PVDF) in N-methyl-2-pyrrolidone (NMP) and the slurry was spread onto a nickel net with 1 cm2 geometry area. The electrode was heated at 100 C for 2 h to evaporate the solvent. Both two-electrode and three-electrode

configurations were used to evaluate the capacitive performances of the electrode materials. In the three-electrode system, a platinum sheet and a standard calomel electrode (SCE) were applied as the counter and reference electrodes, respectively. The mass of active material on the working electrode was about 0.3 mg for the three-electrode system. The accuracy of electronic balance is 0.01 mg (Mettler Toledo AB135-S). The electrolyte was 1 M Na2SO4 aqueous solution. Cyclic voltammetry and electrochemical impedance spectroscopy (EIS) measurements were carried out by a CHI 660C electrochemical workstation. The EIS was measured in the frequency range of 10 mHze100 kHz at an open-circuit potential with an AC amplitude of 5 mV. The obtained datawas fitted to an equivalent circuit model using ZWiew software. Galvanostatic charge discharge test was performed by an Arbin MSTAT4 multichannel galvanostat/potentiostat.

RESULTS AND DISCUSSIONS

Preparation of Rice Husk Based–Carbon and Activated Carbon

Preparation rice husk based–carbon and activated carbon was carried out by burning rice husk up to temperature of 300°C and 400°C. Characterization was including ash content determination. Surface characteristics were determined by X-Ray Fluorescence (XRF) and X-Ray Diffraction (XRD). The results of the characterization of rice husk based activated carbon (KASP) provide information about changes in the carbon and rice husk based activated carbon.

Ash content

The percentage of mineral content of rice husk as raw material for the production of activated carbon can be determined by measuring the ash content. Ash content is closely related to the mineral content. The higher the mineral content, the higher the ash content. The results of ash assay from rice husk which was burnt at a temperature of 750 °C for 4 hours is shown in Table 1.

Tabel 1 : The results of rice husk ash measurements after burning at a temperature of 750 ^{o}C for 4 hours

No.	Cup weight (g)	Rice husk weight (g)	Weight before combustion (g)	Total weight after combustion (g)	Weight balance (g)	% ash content
1	31,812	8,068	39,880	33,382	1,570	19,460
2	27,473	8,080	35,553	29,266	1,793	22,191
3	34,012	8,093	42,105	35,603	1,591	19,659

The measurement results show that the ash content or the average mineral content of rice husk is 20.436%. The mineral content of 20.436% indicates that many minerals are contained in rice husks.

Activated carbon of combustion products at temperature of 750 °C for 4 hours is shown in Figure 1. Color indicates that the carbon content in the activated carbon is smaller than the content of silica.

Figure 1. Rice husk combustion products at a temperature of 750 ° C for 4 hours

MnO2 nanoparticle synthesis through redox deposition

In this research, synthesis of nanocomposite MnO2/KASP in a solution containing KMnO4 and KASP through heterogenic nucleation of MnO2 on the surface of rice husk based activated carbon. The preliminary proof that we have is on the changing of diffraction pattern before and after deposition MnO2 on the surface of rice husk based activated carbon. This will be discussed further in the following section. Morphology MnO2 which is grown on the surface of KASP was also changing from nanorod into nanoparticles when the ratio of KASP/KMnO4 is lowered.

Surface characterization by X-Ray Fluoresence

XRF, or X-Ray Flouresence is a method of surface analysis to determine the surface characteristics of a material, which in this study is the carbon generated by carbonization of rice husk at a temperature of 400 C. The result of XRF analysis for rice husk based carbon before and after the addition of KMnO4 is given in Table 2 and Table 3.

Table 2. XRF data of rice husk based activated carbon (KASP) before MnO2 deposition.

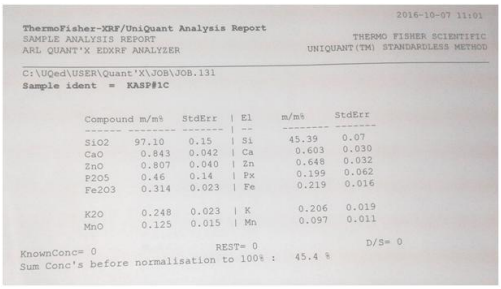

2016-10-07 11:01

ThermoFisher-XRF/UniQuant Analysis Report
SAMPLE ANALYSIS REPORT
ARL QUANT'X EDXRF ANALYZER

THERMO FISHER SCIENTIFIC
UNIQUANT(TM) STANDARDLESS METHOD

C:\UQed\USER\Quant'X\JOB\JOB.131
Sample ident = KASP#1C

Compound	m/m%	StdErr	El	m/m%	StdErr
SiO2	97.10	0.15	Si	45.39	0.07
CaO	0.843	0.042	Ca	0.603	0.030
ZnO	0.807	0.040	Zn	0.648	0.032
P2O5	0.46	0.14	Px	0.199	0.062
Fe2O3	0.314	0.023	Fe	0.219	0.016
K2O	0.248	0.023	K	0.206	0.019
MnO	0.125	0.015	Mn	0.097	0.011

KnownConc= 0 REST= 0 D/S= 0
Sum Conc's before normalisation to 100% : 45.4 %

Table 3. XRF data of rice husk based activated carbon (KASP) after MnO2 deposition.

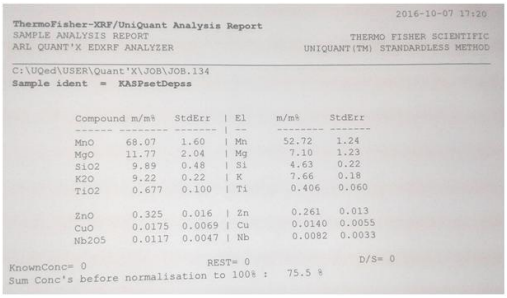

2016-10-07 17:20

ThermoFisher-XRF/UniQuant Analysis Report
SAMPLE ANALYSIS REPORT
ARL QUANT'X EDXRF ANALYZER

THERMO FISHER SCIENTIFIC
UNIQUANT(TM) STANDARDLESS METHOD

C:\UQed\USER\Quant'X\JOB\JOB.134
Sample ident = KASPsetDepss

Compound	m/m%	StdErr	El	m/m%	StdErr
MnO	68.07	1.60	Mn	52.72	1.24
MgO	11.77	2.04	Mg	7.10	1.23
SiO2	9.89	0.48	Si	4.63	0.22
K2O	9.22	0.22	K	7.66	0.18
TiO2	0.677	0.100	Ti	0.406	0.060
ZnO	0.325	0.016	Zn	0.261	0.013
CuO	0.0175	0.0069	Cu	0.0140	0.0055
Nb2O5	0.0117	0.0047	Nb	0.0082	0.0033

KnownConc= 0 REST= 0 D/S= 0
Sum Conc's before normalisation to 100% : 75.5 %

Table 2 provides information on surface composition of rice husk activated carbon before the addition of KMnO4. From the table it can be known that silica is the most dominant species on the surface of the carbon that is also influential in the reaction with KMnO4 when compared to commercial activated carbon. It can be seen that the main composition is SiO2 (97% m/m). Table 3 provides information on the surface composition of rice husk based activated carbon (KASP) after the addition of KMnO4. It can be seen that the presence of manganese (in the form of MnO) is the major component after KMnO4 addition to KASP. This is a proof that the reduction of MnO_4^- (Mn^{+7}) to the lower oxidation state takes place according to the following reaction. Verification whether the final oxidation state of manganese is +4 (MnO_2) or +2 (MnO) will be shown in the result of XRD analysis.

$$4\ KMnO_4 + 3C + H_2O \rightarrow 4MnO_2 + K_2CO_3 + 2\ KHCO_3$$

It should be noted that XRF gives the same response to a metal regardless of its oxidation state in compounds, e.g XRF provides the same information to the manganese compound the following oxidation state: MnO2 (oxidation number +4)

and MnO (+2 oxidation number) as shown in Figure 2. Information on oxidation numbers can be detected using spectroscopic techniques XPS (X-Ray Photoelectron Spectroscopy) or see manganese diffraction data (XRD) as contained in the reference.

X-Ray Diffraction Analysis

The burning of rice husk at a controlled and high temperature produced activated carbon as a source of amorphous silica in the form of $(Na_2O)_m(SiO_2)_n$. This can be seen in the presence of strong diffraction peak between 2θ = 20-30° as shown in the diffraction pattern of KASP in Figure 3. This peak is specific for SiO2 peak as also confirmed in the previous literature. Peak data are given in Table 4.

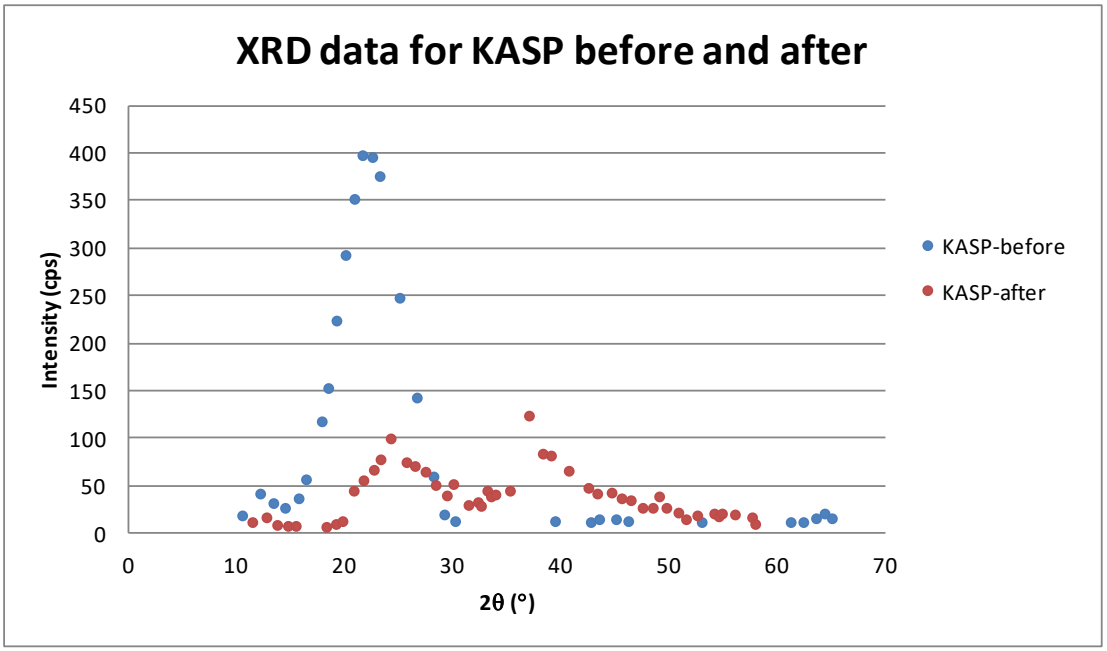

Figure 3. XRD data of rice husk based activated carbon (KASP) before and after the addition of KMnO4

Tabel 4. XRD data profile of KASP before $KMnO_4$ addition

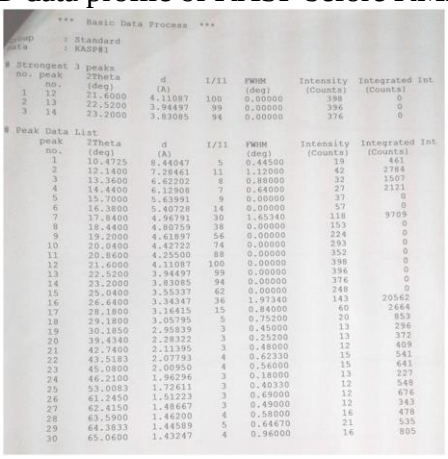

*** Basic Data Process ***

Group : Standard
Data : KASP#1

Strongest 3 peaks

no.	peak no.	2Theta (deg)	d (A)	I/I1	FWHM (deg)	Intensity (Counts)	Integrated Int (Counts)
1	12	21.6000	4.11087	100	0.00000	398	0
2	13	22.5200	3.94497	99	0.00000	396	0
3	14	23.2000	3.83085	94	0.00000	376	0

Peak Data List

peak no.	2Theta (deg)	d (A)	I/I1	FWHM (deg)	Intensity (Counts)	Integrated Int (Counts)
1	10.4725	8.44047	5	0.44500	19	461
2	12.1400	7.28461	11	1.12000	42	2784
3	13.3600	6.62202	8	0.88000	32	1507
4	14.4400	6.12908	7	0.64000	27	2121
5	15.7000	5.63991	9	0.00000	37	0
6	16.3800	5.40728	14	0.00000	57	0
7	17.8400	4.96791	30	1.65340	118	9709
8	18.4400	4.80759	38	0.00000	153	0
9	19.2000	4.61897	56	0.00000	224	0
10	20.0400	4.42722	74	0.00000	293	0
11	20.8600	4.25500	88	0.00000	352	0
12	21.6000	4.11087	100	0.00000	398	0
13	22.5200	3.94497	99	0.00000	396	0
14	23.2000	3.83085	94	0.00000	376	0
15	25.0400	3.55337	62	0.00000	248	0
16	26.6400	3.34347	36	1.97340	143	20562
17	28.1800	3.16415	15	0.84000	60	2664
18	29.1800	3.05795	5	0.75200	20	853
19	30.1850	2.95839	3	0.45000	13	296
20	39.4340	2.28322	3	0.25200	13	372
21	42.7400	2.11395	3	0.48000	12	409
22	43.5183	2.07793	4	0.62330	15	541
23	45.0800	2.00950	4	0.56000	15	641
24	46.2100	1.96296	3	0.18000	13	227
25	53.0083	1.72611	3	0.40330	12	548
26	61.2450	1.51223	3	0.69000	12	676
27	62.4150	1.48667	3	0.49000	12	343
28	63.5900	1.46200	4	0.58000	16	478
29	64.3833	1.44589	5	0.64670	21	535
30	65.0600	1.43247	4	0.96000	16	805

The results of measurements of activated carbon shown in Figure 3 has a widened peak with a peak value of silica is the strongest at the 2θ = 20-30o (d = 3.71) with a degree of crystallinity of 52.4165%. The peak value is only one on KASP indicates that the active carbon is more amorphous.

The highlight of silica decreased dramatically after the addition of $KMnO_4$ is likely a reaction other than the alleged previous reaction.

$$4\ KMnO_4 + 3C + H_2O \rightarrow 4MnO_2 + K_2CO_3 + 2\ KHCO_3 \quad (2)$$

New peak in the area of 2theta = 37° indicate the formation of MnO2 compounds on the surface of KASP as shown in Figure 3 or peak information as given in Table 5.

Table 5. XRD data profile of KASP after KMnO4 addition

*** Basic Data Process ***

Group : Standard
Data : KASPsetDepss

Strongest 3 peaks

no.	peak no.	2Theta (deg)	d (A)	I/I1	FWHM (deg)	Intensity (Counts)	Integrated Int (Counts)
1	27	37.0200	2.42637	100	1.55000	124	10735
2	13	24.2200	3.67178	81	0.00000	100	0
3	28	38.3000	2.34817	68	0.00000	84	0

Peak Data List

peak no.	2Theta (deg)	d (A)	I/I1	FWHM (deg)	Intensity (Counts)	Integrated Int (Counts)
1	11.4100	7.74898	10	0.50000	12	317
2	12.7200	6.95373	14	0.40000	17	476
3	13.7100	6.45374	7	0.22000	9	156
4	14.7070	6.01840	6	0.32600	8	132
5	15.4350	5.73614	6	0.29000	8	179
6	18.2600	4.85458	6	0.04000	7	36
7	19.1500	4.63092	8	0.38000	10	237
8	19.7600	4.48931	10	0.44000	13	361
9	20.8000	4.26714	36	0.86660	45	2878
10	21.7000	4.09215	45	0.00000	56	0
11	22.6600	3.92091	54	0.00000	67	0
12	23.2800	3.81787	63	0.00000	78	0
13	24.2200	3.67178	81	0.00000	100	0
14	25.6800	3.46624	60	0.00000	75	0
15	26.4600	3.36580	57	0.00000	71	0
16	27.4400	3.24778	52	0.00000	65	0
17	28.3800	3.14231	41	0.00000	51	0
18	29.4200	3.03355	32	0.00000	40	0
19	30.0200	2.97427	42	0.98280	52	3460
20	31.4200	2.84487	24	0.00000	30	0
21	32.3000	2.76934	27	0.00000	33	0
22	32.5800	2.74618	23	0.00000	29	0
23	33.1600	2.69946	36	0.00000	45	0
24	33.5000	2.67283	31	0.00000	39	0
25	33.9200	2.64069	33	0.92000	41	1760
26	35.2600	2.54334	36	1.20000	45	2895
27	37.0200	2.42637	100	1.55000	124	10735
28	38.3000	2.34817	68	0.00000	84	0
29	39.0600	2.30422	66	0.00000	82	0
30	40.7000	2.21507	53	1.59000	66	8180
31	42.5200	2.12438	39	0.76000	48	1682
32	43.3400	2.08606	34	1.32000	42	2195
33	44.6683	2.02707	35	0.56330	43	1209
34	45.5900	1.98820	30	0.54000	37	1060
35	46.4450	1.95357	28	0.51000	35	1124
36	47.5350	1.91129	22	0.51000	27	943
37	48.4800	1.87622	22	0.26000	27	415
38	49.0700	1.85503	31	0.86000	39	1118
39	49.7400	1.83160	22	0.76660	27	899
40	50.8486	1.79424	18	0.48930	22	551
41	51.5546	1.77132	12	0.15730	15	159
42	52.6000	1.73855	15	0.36000	19	603
43	54.1650	1.69195	17	0.55000	21	774
44	54.5800	1.68006	15	0.00000	18	0
45	54.8864	1.67141	17	0.24710	21	528
46	56.0866	1.63845	16	0.18670	20	329
47	57.6750	1.59705	14	0.21000	17	303
48	57.9600	1.58987	8	0.12000	10	114

XRD data to synthesized MnO2 showed that the sample was amorphous which was explained by the presence of wide peak in the area 2theta= 30-40° (Tomko et al, 2011). Other supporting data can be seen in Figure 5 (Wang et al. 2011).

As seen in Figure 5, the XRD patterns of MnO2 nanoparticles showed a clear peak and width at 37° and 65°, which therefore indicates that the sample is less crystalline (JCPDS No. 44-0141). Wide reflection shows that the particle size of the sample was small.

From this explanation, it can be concluded that manganese has been reduced from oxidation state +7 (MnO4-) to +4 (MnO2), not to +2 (MnO) as shown in the previous XRF results.

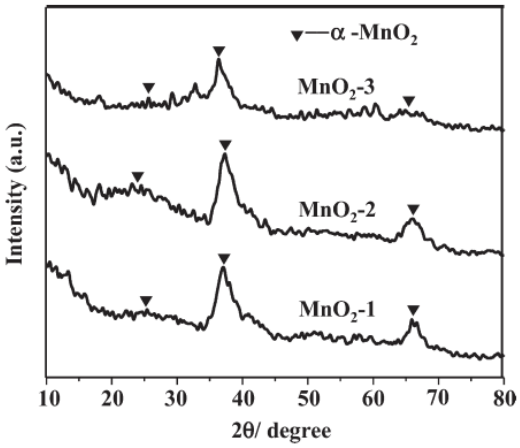

Figure 5. Diffraction data of MnO2 compound indicated by peak at 2theta = 3737° ((Wang, et al. 2011).

Figure 6 shows the voltammogram profile of commercially activated carbon (KAK) and rice husk based activated carbon (KASP) before and after MnO2 deposition. The most symmetric voltammogram is shown by electrode which is constructed from KASP material.

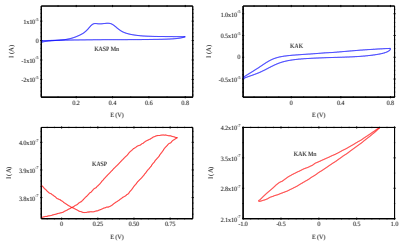

Figure 6. Cyclic voltammogram profile of KASP and KAK before and after deposition of MnO2. KASP-Mn = Rice husk based activated carbon after MnO2 deposition, KAK = commercial activated carbon, KAK-Mn = KAK after MnO2 deposition.

Tabel 6 Spesific capacitance of KAK and KASP based pseudo-capacitor electrode (before and after MnO2 deposition).

No	Sample	Specific Capacitance
1	KAK (Commercially AC)	33 μF/g
2	KAK-MnO2 (composite CAC-MnO2)	29,6 mF/g
3	KASP (Rice Husk Based AC)	8,6 μF/g
4	KASP-MnO2 (composite KASP-MnO2)	25,4 mF/g

From that table, it can be seen that there is a significance increase in Cs after MnO2 deposition, either in electrode constructed from KAK or KASP. For electrode developed using KAK, there is an increase ± 1000 times after the presence of MnO2 on the surface of commercially activated carbon. For electrode developed using KASP, there is an increase ± 3000 times after the presence of MnO2 on the surface of rice husk based activated carbon. This suggests that agricultural waste based activated carbon has a better performance than commercially activated carbon. KAK is more expensive in price than KASP. However, it should be confessed that the order of capacitance obtained in this study is low, in the order of mikro- to milli- Farad compared to the previous research. This results adaptate with the facility in our lab, for example in the construction of pseudo-capacitor electrode.

The increase in the capacitance can be explained by the pseudocapacitive effect of MnO2 on the surface of both carbons. This also suggests that there is a very significant improvement on functional properties of carbon material which is obtained from biomass based agricultural waste. The improvement in the functional properties of electrode material will also increase the performance of pseudo-capacitor as shown in Table 6. This will be an value-added of this research since we employ an agricultural waste which is in a huge amount around us, and sometimes causes enviromental pollution.

CONCLUSIONS

Nanocomposite MnO2/Rice Husk based Activated Carbon (KASP) has been synthesized by means of one-step chemical synthesis in a solution containing KMnO4 and KASP via heterogenic nucleation of MnO2 nanoparticles on the surface of activated. If the reaction ratio KASP/KMnO4 is changing, morphology of MnO2 that grows on the surface of KASP also changed from nanorod to nanoparticles.

A pseudo-capacitor with high energy density was fabricated by using MnO_2/KASP nanocomposite as positive electrode and activated carbon as negative electrode in 1 M Na_2SO_4 aqueous electrolyte. The pseudocapacitor can be cycled reversibly in the cell voltage of 0.2 V, and delivers a specific capacitance of $25.4\ mF\ g^{-1}$ (based on the total mass of active electrode materials of 9.4 mg), which is much higher than that of supercapacitor without MnO_2 deposition ($8.6\ \mu F\ g^{-1}$), or there is significance increase in capacitance (± 3000 times). We obtained also that rice husk based activated carbon has a better performance compared to commercially activated carbon material.

Such good electrochemical performance makes nanocomposite MnO2/KASP as a promising electrode material for supercapacitors.

ACKNOWLEDGEMENTS

Acknowledgments for financial assistance through the Fund of BOPTN Hasanuddin University in 2016 in accordance with the Agreement of Implementation No: 1454 / UN4.20 / P / L.09 / 2016.

REFERENCES

Bagotsky, V.S. Skundin, A.M. Volfkovich, Y.M. **2015**, "*Electrochemical power sources: batteries, fuel cells, and supercapacitors*", John Wiley & Sons, Inc.

Beguin, F. Frackowiak, E. (Eds.). 2010. *Carbons for Electrochemical Energy Storage and Conversion Systems*, CRC Press, Taylor & Francis Group, Boca Raton, FL. ISBN 978-1-4200-5307-4.

Beguin, F. Presser, V. Balducci, A. Frackowiak, E. **2014**. *"*Carbon and Electrolytes for Advanced Supercapacitors (Review)", *Adv. Mater*., 1-33. DOI: 10.1002/adma.201304137. Wiley-VCH Verlag GmbH&Co. KgaA, Weinheim.

Chen, M.D. Wumale, T. Li, W.L. Song, H.H., Song, R.R. **2015**, "Electrochemical performance of cotton stalk based activated carbon electrodes modified by MnO_2 for supercapacitor", *Mat. Tech*., Vol 30, pp. A2-A7.

Caballero, A. Hernan, L. Morales, J. 2011. Limitations of Disordered Carbons Obtained from Biomass as Anodes for Real Lithium-Ion Batteries, *Chem. Sus. Chem*., 4, 658-663.

Chen, H. Zeng, S. Chen M. Zhang, Y. Zheng L. Li, Q. **2016**, "Oxygen evolution assisted fabrication of highly loaded carbon nanotube/MnO_2 hybrid films for high performance flexible pseudosupercapacitors", *Small Nano Micro*, 12(15) pp. 2035-2045.

Chen, Y. Zhu, Y. Wang, Z. Li, Y. Wang, L. Ding, L. Gao, X. Ma, Y. Guo, Y. 2011. "Application studies of activated carbon derived from rice husks produced by chemical-thermal process – a review", *Adv. Coll. Inter. Sci*., 163, 39-52.

Daubert, J.S. Lewis, N.P. Gotsch, H.N. Mundy, J.Z. Monroe,D.N. Dickey, E.C. Losego, M.D. Parsons, G.N. **2015**, "Effect of meso- and micro-porosity in carbon electrodes on atomic layer deposition of pseudocapacitive V_2O_5 for high performance supercapacitors, *Chem. Mater*., 27(19), pp. 6524-6534, DOI:10.1021/acs.chemmater.5b01602

Dutta, S. Bhaumik, A. Wu, K.C.W. **2014**,"Hierarchichally porous carbon derived from polymers and biomass: effect of interconnected pores on energy application (review)", *Energy Environ. Sci*., 7, 3574-3592.

Frackowiak, E. Beguin, F. 2001. "Carbon materials for the electrochemical storage of energy in capacitors (review)". *Carbon*. 39(937-950).

Frackowiak, E. Beguin, F. 2002. "Electrochemical storage of energy in carbon nanotubes and nanostructured carbons". *Carbon*. 40(1775-1787).

He, X. Ling, P. Qiu, J. Yu, M. Zhang, X. Yu, C. Zheng, M. **2013**. "Efficient preparation of biomass-based mesoporous carbons for supercapacitors with both high energy density and high power density", *J. Power Sources*, 240, 109-113.

Ioannidou, O. Zabaniotou, A. 2007."Agricultural residues as

precursor for activated carbon production-a review". *Renewable & Sustainable Energy Reviews*. 11(1966-2005).

Kalyani, P. Anitha, A. **2013**. "Biomass Carbon and Its Prospects in Electrochemical Energy Systems (Review)", *Int. J. Hydrogen Energy*, 38, 4034-45.

Lai, F. Miao, Y. Huang, Y. Chung, T.S. Liu, T. **2015**, "Flexible hybridmembranes of NiCo2O4-doped carbon nanofiber-MnO2 core-sheath nanostructures for high performance supercapacitors", *J. Phys. Chem. C*, 119(24), pp. 13442-13450.

Li, D. Yang, D. Quan, F. Wang, B. Zhang, L. Zhu, S. Wang, L. **2015**, "Carbon fibers coated with metal oxides nanostructures as electrode materials for energy storage devices", *Nano Reports*, 2015, 1, 29-41.

Li, X. Xing, W. Zuo, S. Zhou, J. Li, F. Qiao, S. Z. Lu, G.Q. **2011**. "Preparation of capacitor's electrode from sunflower sheed shell". *Bioresour. Technol*. 102 (1118–1123).

Ma, G. Yang, Q. Sun, K. Peng, H. Ran, F. **2015**,"Nitrogen-doped porous carbon derived from biomass waste for high performance supercapacitor", *Bioresource Tech*. 2015, 197, 137-142.

Manik, S.T. Taer, E. Iwantono, **2013**, "*Impedansi Spektroskopi Sel Superkapasitor menggunakan Elektroda karbon bentuk monolit dari ampas tebu"*, Jurnal On Line Mahasiswa MIPA Universitas Riau.

Nabais, J.V. Carrott, P. Ribeiro Carrott, M.M.L. Luz, V. Ortiz, A.L. 2008. "Influence of preparation conditions in the textural and chemical properties of activated carbons from a novel biomass precursor: the coffee endocarp". *Bioresour. Technol*. 99 (7224–7231).

Pandolfo, A.G. Hollenkamp, A.F. 2006. "Carbon properties and their role in supercapacitors". *J. Power Sources*. 157(11-27).

Raymundo-Piñero, E. Leroux, F. Béguin, F. 2006. "A high-performance carbon for supercapacitors obtained by carbonization of a seaweed biopolymer". *Adv. Mater*. 18 (1877–1882).

Rosi, M. Ekaputra, M.P. Iskandar, M. Abdullah, M. Khairurrijal, 2012, "*Superkapasitor Menggunakan Polimer Hidrogel Elektrolit dan Elektroda Nanopori Karbon"*, Prosiding SEMNAS Material, Fisika, ITB.

Rufford, T.E. Hulicova-Jurcakova, D. Zhu, Z.H. Lu, G.Q. 2008. "Nanoporous carbon electrode from waste coffee beans for high performance supercapacitors". *Electrochem. Commun*. 10(1594–1597).

Rufford, T.E. Hulicova-Jurcakova, D. Khosla, K. Zhu, Z., Lu, G.Q. **2010**. "Microstructure and electrochemical double-layer capacitance of carbon electrodes prepared by zinc chloride activation of sugar cane bagasse". *J. Power Sources* 195 (912–918).

Salunkhe, R.R. Ahn, H. Kim, J.H. Yamauchi, Y. 2015, "Rational design of coaxial structured carbon nanotube–manganese oxide (CNT–MnO2) for energy storage application", *Nanotechnology*, 26, 7pp, doi:10.1088/0957-4484/26/20/204004

Sekine, T. dan Zakir, M. 2008. "Oxidative Dissolution of Tc(IV)O2 •nH2O Colloids by Sonolysis".

Radiochim. Acta. 96 (9-11, 625-629).

Simon, P. Gogotsi, Y. 2008. "Materials for electrochemical capacitors (review)". *Nature Mat*. 7 (845-855).

Syarif, N. **2014**. "*Pengembangan kapasitor lapis ganda elektrokimia dari karbon aktif kayu gelam"*, Disertasi, Universitas Indonesia

Taer, E. Sugianto, Sumantre, M.A. Tsalim, R, Iwantono, Dahlan, D. **2013**, "*Pengaruh Ukuran Serat dan Ketebalan Membran Kulit Telur Sebagai Separator Alami pada Pengukuran Cas dan Discas dengan rapat arus yang berbeda terhadap rapat rapat energi dan daya sel superkapasitor"*, Prosiding SEMNAS Fisika Univ. Andalas (SNFUA), ISBN 978-879-25-1954-9

Wang, J. Xin, H.L. Wang, D. **2013**. *"*Recent Progress on Mesoporous Carbon Materials for Advanced Energy Conversion and Storage (Review)", *Part. Part. Syst. Charact*., 1-25. DOI: 10.1002/ppsc.201300315. Wiley-VCH Verlag GmbH&Co. KgaA, Weinheim.

Wang, Y. T. Lu, A.H. Zhang, H.L. Li, W.C. 2011, "Synthesis of Nanostructured Mesoporous Manganese Oxide with Three-Dimensional Frameworks and Their Application in Supercapacitors", *J. Phys. Chem*. C 2011, 115, 5413-5421.

Wei, L. Yushin, G. **2012**."Nanostructured activated carbon from natural precursors for electrical double layer capacitors (review)", *Nano Energy*, 1, 552-565.

Winter, M. Brodd, R.J. 2004. "What are batteries, fuel cells, and supercapacitors? (review)" *Chem. Rev*. 104(4245-4269).

Wu, F.C. Tseng, R.L. Hu, C.C. Wang, C.C. 2004. "Physical and electrochemical characterization of activated carbons prepared from firewood for supercapacitors". *J. Power Sources* 138(351–359).

Xie, J. Sun, X. Zhang, N. Xu, K. Zhou, M. Xie, Y. **2013**."Layer by layer beta-Ni(OH)2/grapheme nanohybrids for ultraflexible all solid state thin film supercapacitors with high electrochemical performance". *Nano Energy*, 2, 65-74.

Xing, W. Qiao, S.Z. Ding, R.G. Li, F. Lu, G.Q. Yan, Z.F. Cheng, H.M. 2006. "Superior electric double layer capacitors using OMC". *Carbon*. 44(216-224).

Xu, P. Wei, B. Cao, Z. Zheng, J. Gong, K. Li, F. Yu, J. Li, Q. Lu, W. Byun, J.H. Kim, B.S. Yan, Y. Chou, T.W. **2015**, "Stretchable Wire-Shaped Asymmetric Supercapacitors Based on Pristine and MnO2 Coated carbon Nanotube Fibers", *ACS Nano*, 9 (6), pp. 6088-6096. DOI:10.1021/acsnano.5b01244

Yang, J. Liu, Y. Chen, X. Hu, Z. Zhao, G. 2008. "Carbon electrode material with high densities of energy and power". *Acta Physica-Chimica Sinica*. 24(13–19).

Yu, A. Chabot, V. Zhang, J. **2013**, "*Electrochemical Supercapacitors for Energy Storage and Delivery: Fundamentals and Applications*", Taylor & Francis Group, LLC.

Zakir, M. dan Sekine, T. 2009. "Oxidation Reaction of $Tc(IV)O_2.nH_2O$ Nanocolloid Induced by Ultrasonic Wave". *Indo. Chim. Acta*. 2 (1, 46-47).

Zakir, M. dan Sekine, T. 2010. "Sonolytic Oxidation of $Tc(IV)O_2.nH_2O$ Nanoparticles to $Tc(VII)O_4$- in

Aqueous Solution". *Atom Indonesia*. 36 (1, 17-22).

Zakir, M. Maming, and Achmad, A. **2011**. "Adsorption of Methylene Blue and Eosin on Rice Husk Based Activated Carbon". *Indo. Chim. Acta*. 4 (2, 1-6).

Zakir, M. Maming, Raya, I. Karim, A. Santi. **2012**. "Pemanfaatan Energi Gelombang Ultrasonik Dalam Adsorpsi Ion Logam Berat Cu(II) pada Bioadsorben Karbon Aktif dari Sekam Padi". *Indo. Chim. Acta*. 5 (2, 1-9).

Zakir, M. **2013**. "*Ultrasound-assisted adsorption of lead(II) and copper(II) ions on rice husk activated carbon*". Proceeding of The International Conference on Quality in Research, Yogyakarta, 25-28 June 2013, pp.

Zakir, M. Botahala, L. Ramang, M. St. Fauziah, Abdussamad, B. **2013**. "Electro-deposition of Mn on the Surface of Rice Husk Based Active Carbon under Sonication". *Indo. Chim. Acta*. 6 (2, 9-18).

Zhang, F. Ma, H. Chen, J. Li, G.D. Zhang, Y. Chen, J.S. 2008. "Preparation and gas storage of high surface area microporous carbon derived from biomass source cornstalks". *Bioresour. Technol*. 99(4803–4808).

Zhang, Y. Xing, H. Wu, X. Wang, L. Zhang, A. Xia, T.C. Dong, H.C. Li, X.F. Zhong, L.S. 2009. "Progress of electrochemical capacitor electrode materials: a review". *Int. J. Hydrogen Tech.* 34 (4889–4899).

Zhang, X. Sun, X. Zhang, H. Zhang, D. Ma, Y. **2012**, "Development of redox deposition of birnessite-type MnO_2 on activated carbon as high-performance electrode for hybrid capacitors", *Mat. Chem. Phys*., 137, 290-296.

Zhou, J. Ji, Y. He, J. Zhang, C. Zhao, G. 2008. "Enhanced mesoporosity and capacitance property of spherical carbon aerogel prepared by associating $Mg(OH)_2$ with non-ionic surfactant". *Micropor. Mesopor. Mater*. 114(424–430).

Zhong, C. Deng, Y. Hu, W. Qiao, J. Zhang, L. Zhang, J. **2015**. "A review of electrolyte materials and compositions for electrochemical supercapacitors". *Chem. Soc. Rev.*, 2015, 44, 7484-7539.